

## Supplementary data

# An oriented Ni-Co-MOF anchored on solution-free 1D CuO: a p-n heterojunction for supercapacitive energy storage

Iftikhar Hussain <sup>a#</sup>, Sarmad Iqbal <sup>b#</sup>, Tanveer Hussain <sup>c#</sup>, Yatu Chen <sup>a</sup>, Muhammad Ahmad <sup>a</sup>,  
Muhammad Sufyan Javed <sup>d</sup>, Akram AlFantazi <sup>b, e</sup>, Kaili Zhang <sup>a\*</sup>

<sup>a</sup> Department of Mechanical Engineering, City University of Hong Kong, 83 Tat Chee Avenue, Kowloon,  
Hong Kong

<sup>b</sup> Department of Chemical Engineering, Khalifa University, Abu Dhabi 127788, United Arab Emirates

<sup>c</sup> School of Chemical Engineering, The University of Queensland, St Lucia, QLD 4072, Australia

<sup>d</sup> School of Physical Science and Technology, Lanzhou University, Lanzhou 730000, China

<sup>e</sup> Nuclear Technology Center, Khalifa University, Abu Dhabi, United Arab Emirates

# Equal Contribution

\*Corresponding author: kaizhang@cityu.edu.hk (Prof. Kaili Zhang)

## **Part I. Experimental section**

### **Materials**

Cobalt nitrate hexahydrate (98%), nickel (II) nitrate hexahydrate (98%), potassium hydroxide (flakes), 2-methylimidazole, and copper nitrate trihydrate were obtained from ACROS Hong Kong Labware. Hydrochloric acid (35%) and ethanol were procured from Anaqua (Hong Kong) Company Limited. All chemicals were used without further purification. Copper mesh was pretreated to remove the impurities and oxide layer from the surface.

### **Preparation of CuO nanowires**

The CuO nanowires were obtained by simple and inexpensive solution-free dry oxidation route as already reported<sup>1</sup> with a slight modifications. CuO nanowires were fabricated by solution-free calcination process. Firstly, the pretreated copper mesh ( $3 \times 5$  cm) was placed in the muffle furnace and heated for 4 h at 500 °C (ramping temperature was 5°C per min). After cooling gradually to room temperature, the copper mesh containing CuO nanowires electrode material was obtained.

### **Preparation of Ni-Co-ZIF@CuO**

The Ni-Co-ZIF@CuO was produced by using facile and inexpensive hydrothermal approach as reported elsewhere<sup>2</sup> with a slight modifications. For the synthesis of Ni-Co-ZIF, 7.5 mmol of 2-methylimidazole (2-MIM) was dissolved in 40 mL DI water and stirred to get solution A, 1.2 mmol of  $\text{Ni}(\text{NO}_3)_2 \cdot 6\text{H}_2\text{O}$  and 2.4 mmole of  $\text{Co}(\text{NO}_3)_2 \cdot 6\text{H}_2\text{O}$  were dissolved in 40 mL of DI water and stirred for 20 minutes to get solution B. Subsequently, solution A and B were hurriedly mixed, as prepared CuO NWs substrate was immersed in the resulting solution and then put in Teflon lined stainless steel autoclave and kept in oven at 60 °C for 8 h. The autoclave was then cooled naturally to room temperature. The substrate was then washed several times with DI water and ethanol, and

dried at 60 °C for 12 h in oven. The as-synthesized oriented Ni-Co-ZIF@CuO was named as Ni-Co-ZIF@CuO.

### **Characterizations**

The images were captured using scanning electron microscopy (SEM, FEI Quanta 450 FEG). The crystallinity of the samples was examined by X-ray diffraction (XRD, Rigaku Smart Lab Bruker D2 Phaser) using CuK $\alpha$  radiation. The elemental composition was evaluated using X-ray photoelectron microscopy (XPS, Physical Electronics PHI 5802) using monochromatized AlK $\alpha$  radiation.

### **Electrochemical measurements**

For the measurement of electrochemical performance, the active materials Ni-Co-ZIF@CuO and CuO (1 cm × 1 cm) were used as a working electrode. The electrochemical measurements were carried out in a 3M KOH aqueous electrolyte using a three-electrode system consisting of a platinum plate as the counter electrode, and Hg/HgO as the reference electrode. Cyclic voltammetry (CV), galvanostatic charge-discharge (GCD) measurements, and electrochemical impedance spectroscopy (EIS) were performed on a CHI 660E electrochemical workstation.

### **Fabrication of device**

The oriented Ni-Co-ZIF@CuO was evaluated for practical use. ASC device was fabricated assembled using Ni-Co-ZIF@CuO as positive electrode, rGO as negative electrode, 3 M KOH as electrolyte and filter paper as a separator. The rGO as negative electrode was prepared by slurry coated method. Briefly, rGO, acetylene black, and PVDF were mixed at a mass ratio of 80:15:5 in NMP. The slurry was coated on Cu mesh (1.0 cm × 1.0 cm) and dried for 12 h. The ASC device was assembled using CR2025 coin-type cells, pressed at 15 MPa for 30 seconds.

### **Simulation methods**

Optimized geometries, electronic structures and work function properties of bare (Ni-Co-ZIF) and CuO decorated (Ni-Co-ZIF@CuO) MOF based electrode materials, were studied by using first-principles density functional theory (DFT) calculations through the Vienna *ab initio* Simulation Package (VASP) code<sup>3,4</sup>. Electron-ion interaction was computed through the projector augmented wave (PAW) methods<sup>5,6</sup>. Generalized gradient approximation (GGA) of Perdew-Burke-Ernzerhof (PBE) were used to describe the electron-electron interactions<sup>7</sup>. We used cut-off energy of 500 eV for the plane-wave basis set. Crustal structures were optimized with energy convergence criterion of 10<sup>-5</sup>, whereas the force criteria of 0.001 eV/Å was used throughout the calculations. Because of the large sizes of bare and CuO-doped Ni-Co-ZIF, we used relatively thinner KPOINT mesh of size 2 x 2 x 2 for the sampling of Brillouin zones under the Monkhorst-Pack scheme<sup>8</sup>. Van der Waals (vdW) correction of DFT-D3 as proposed by Grimme et al. was considered on the top of DFT energies<sup>9</sup>.

## **Part II. Calculations**

### **Specific capacity calculation**

The specific capacity was calculated by using the following equation:<sup>10-12</sup>

$$C = \frac{2I\int Vdt}{m v} \quad \text{eq. S1}$$

where C (C g<sup>-1</sup>) is the specific capacity; I (A) is the current during the discharge process; dt (s) is the discharge time; and m (g) is the mass of the active materials.

### **Coulombic efficiency calculation**

The Coulombic efficiency was calculated by using the following equation:

$$\eta(\%) = \frac{td}{tc} \quad \text{eq. S2}$$

Where  $\eta(\%)$  is Coulombic efficiency,  $t_d$  (s) represented discharging time, and  $t_c$  (s) represented charging time.

### **Electrode mass calculation**

To obtain the optimal electrochemical results, the mass ratio between the positive and negative electrode was balanced by using the following equation<sup>10-13</sup>:

$$\frac{m_+}{m_-} = \frac{C_- \Delta V_-}{C_+ \Delta V_+} \quad \text{eq. S3}$$

where  $C_+$  and  $C_-$  are the corresponding specific capacitances of the positive and negative electrodes respectively;  $\Delta V_-$  and  $\Delta V_+$  denote the potential window for the electrodes; and  $m_+$  and  $m_-$  presents the mass of electrode materials.

### **Energy and power density**

The energy and power densities were calculated by the following equations<sup>10, 11, 14</sup>.

$$E = \frac{I \int V dt}{m} \quad \text{eq. S4}$$

$$P = \frac{E}{\Delta T} \quad \text{eq. S5}$$

where  $E$  ( $\text{W h kg}^{-1}$ ) and  $P$  ( $\text{W kg}^{-1}$ ) are the energy density and the power density, respectively.

### **Capacitance envelope calculation**

The current due to capacitance is directly proportional to the scan rate ( $v$ ) and the diffusion-dominated it is proportional to the square root of the scan rate ( $v^{1/2}$ ). In electrochemical measurements with both diffusive and capacitive components, current is proportional to the scan rate raised to the power  $b$ .

$$i = c \times v^b \quad \text{eq. S6}$$

where  $c$  is constant, and the value of  $b$  is between 0.5 and 1.

This contribution of both diffusions limited current and capacitive current can be stated as weight fraction between the two components, where  $x$  is the fraction of total current that is capacitive in nature. Rearranging the equation to find  $x$ :

$$xv + (1 - x)v^{0.5} = v^b \quad \text{eq. S7}$$

$$x = \frac{v^b - 0.5 - 1}{v^{0.5} - 1} \quad \text{eq. S8}$$

and  $b$  can be found by rearranging  $i = c \times v^b$

$$\log(i) = b \times \log(v) + \log(c) \quad \text{eq. S9}$$

The slope of  $\log(i)$  vs  $\log(v)$  being equal to  $b$ . By calculating  $b$  at all potentials and plugging them into equation S8, the capacitive current contribution was obtained and plotted as shown in Fig. 4b.

### Part III. Supplementary images

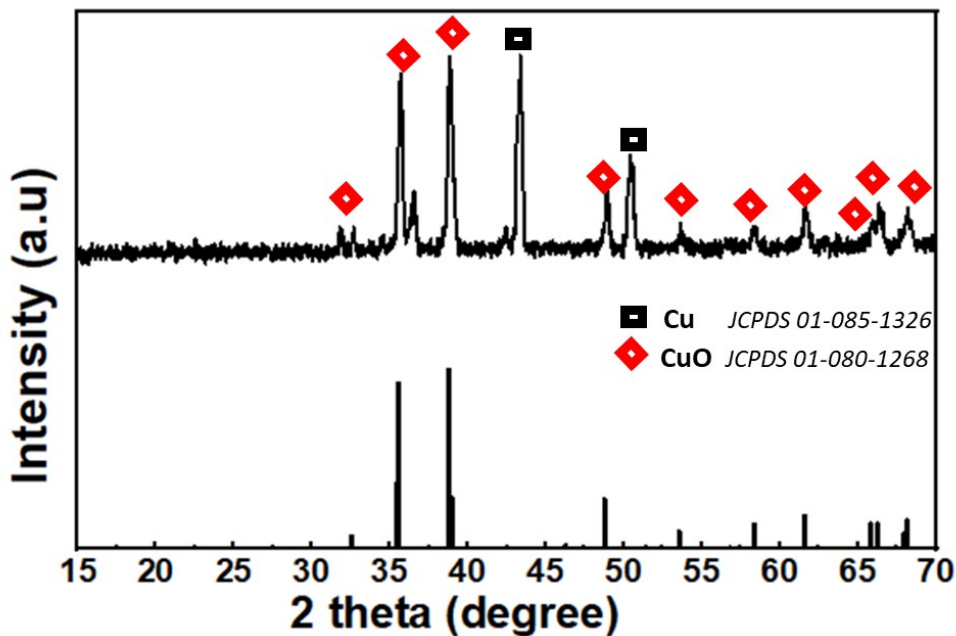


**Figure S1** XRD pattern of CuO NWs.

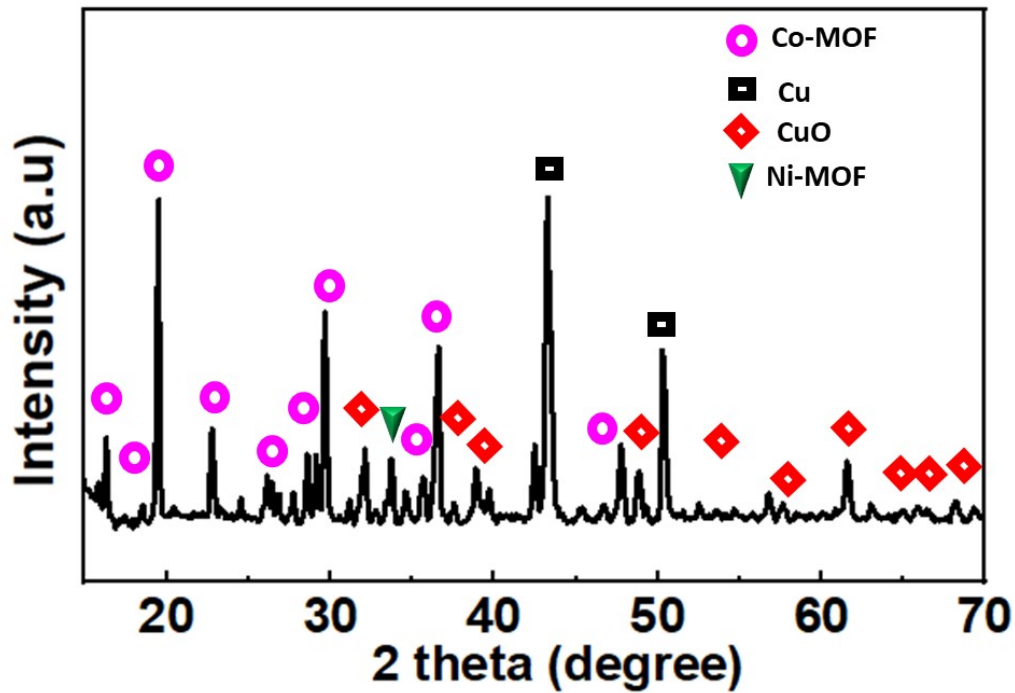


**Figure S2** XRD pattern of Ni-Co-ZIF@CuO.

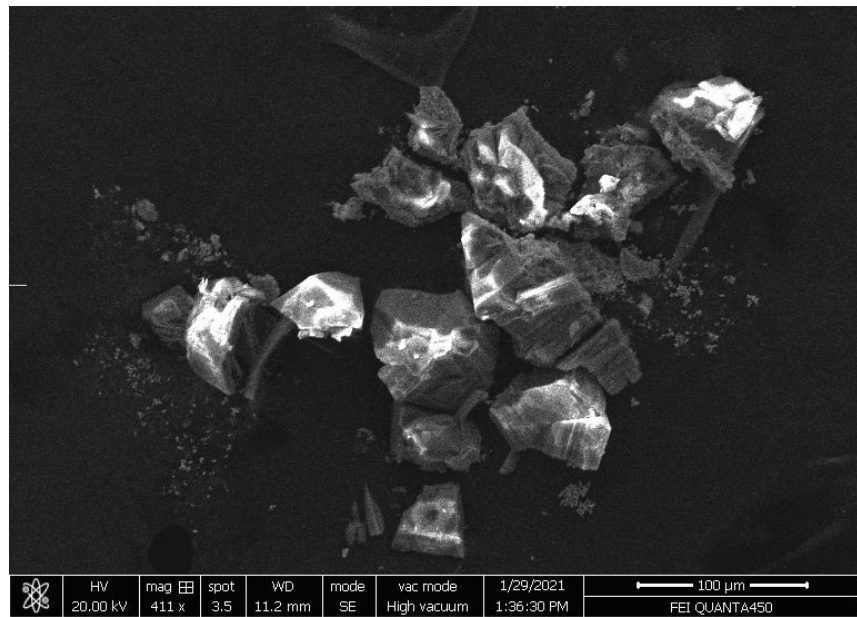


**Figure S3** SEM image of substrate free Ni-Co-ZIF-P.

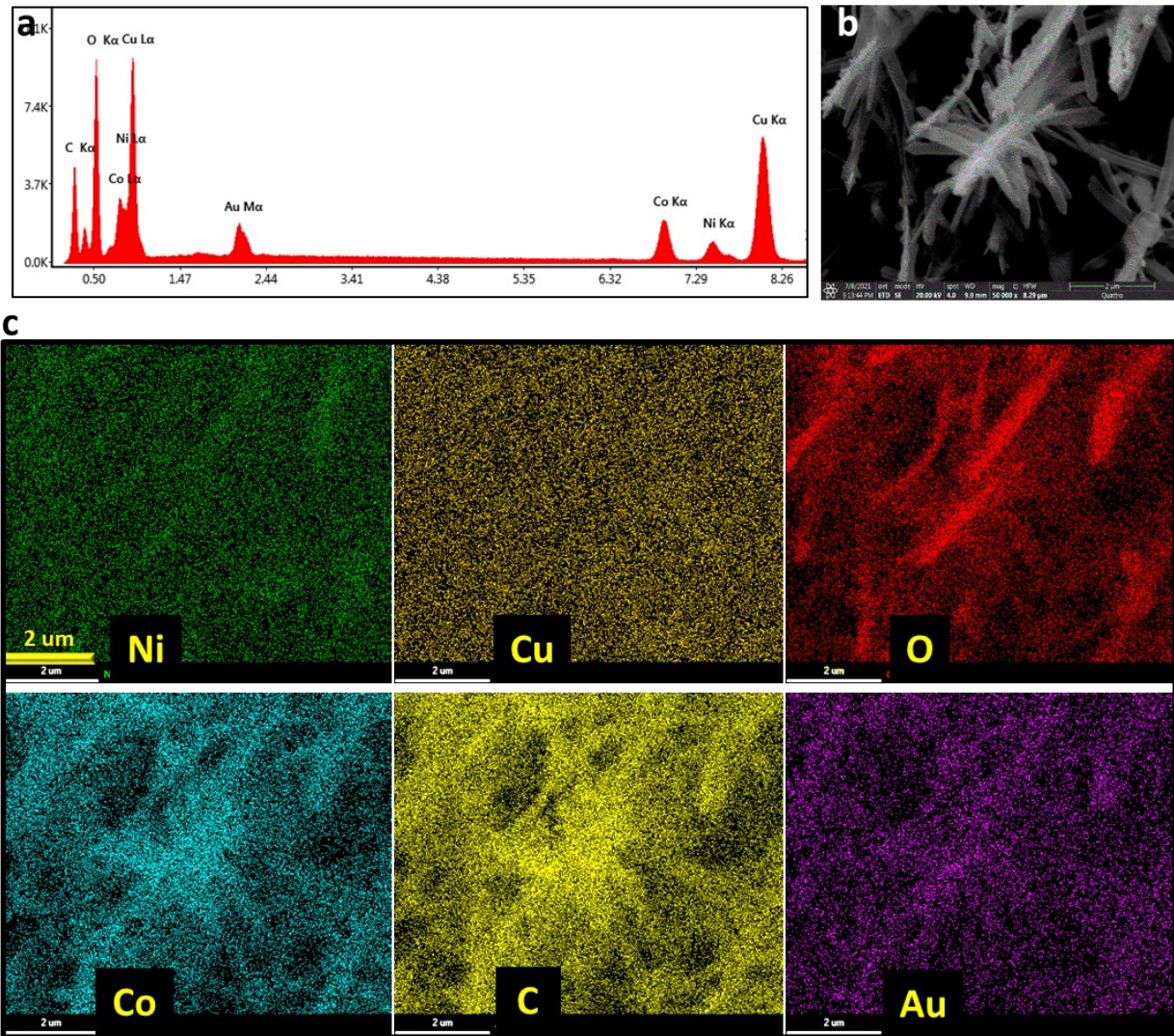


**Figure S4** (a) EDX spectra of Ni-Co-ZIF@CuO, (b) SEM image, and (c) high-resolution elemental mapping for NI, Cu, O, Co, C, and Au. The Au was used as part of the SEM imaging preparation.

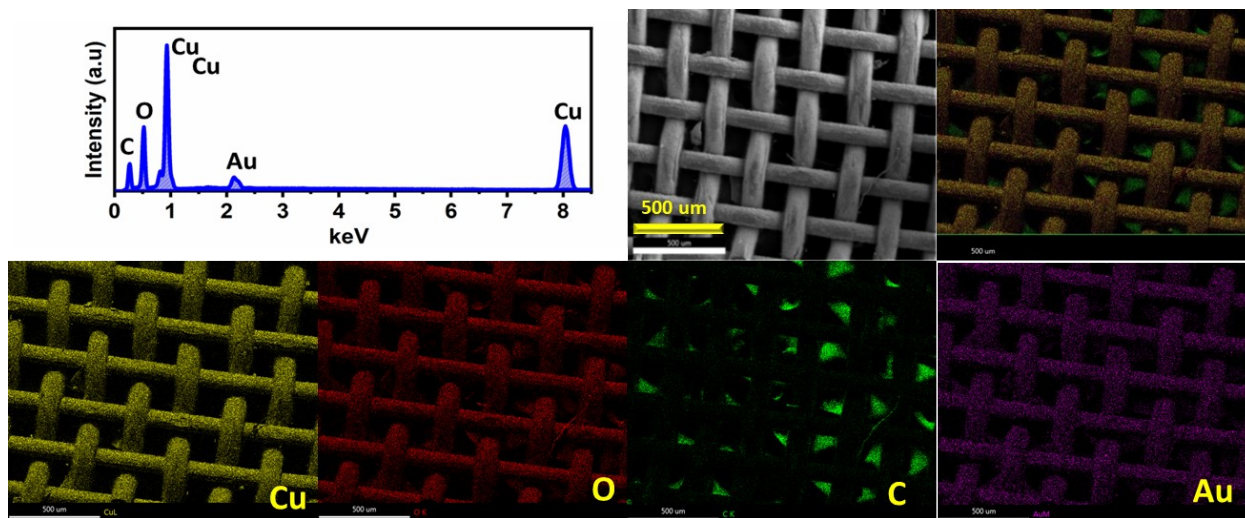


**Figure S5** EDX spectra of CuO NWs, SEM image and elemental mapping for overlay, Cu, O, C and Au. The Au was used as part of the SEM imaging preparation.

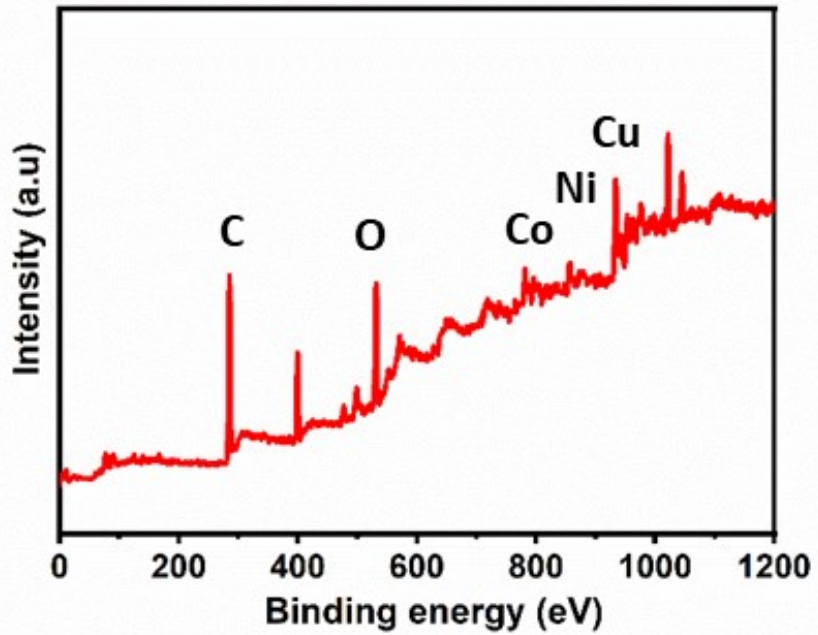


**Figure S6** XPS survey spectra of Ni-Co-ZIF@CuO.

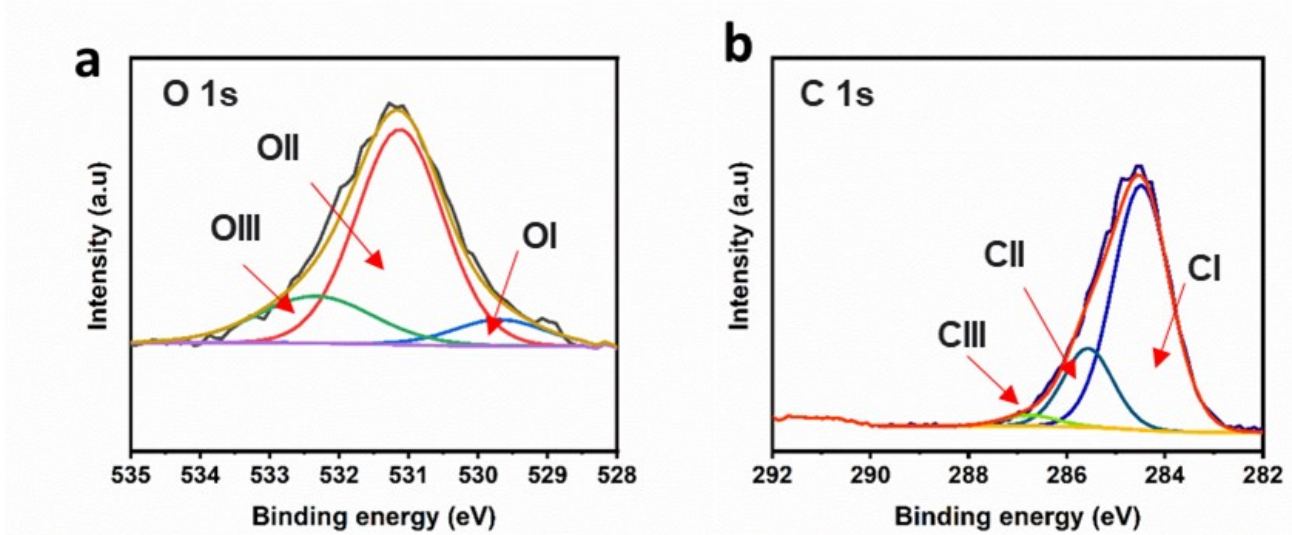


Figure S7 (a) XPS survey spectra of Ni-Co-ZIF@CuO (a) O 1s and (b) C 1s.

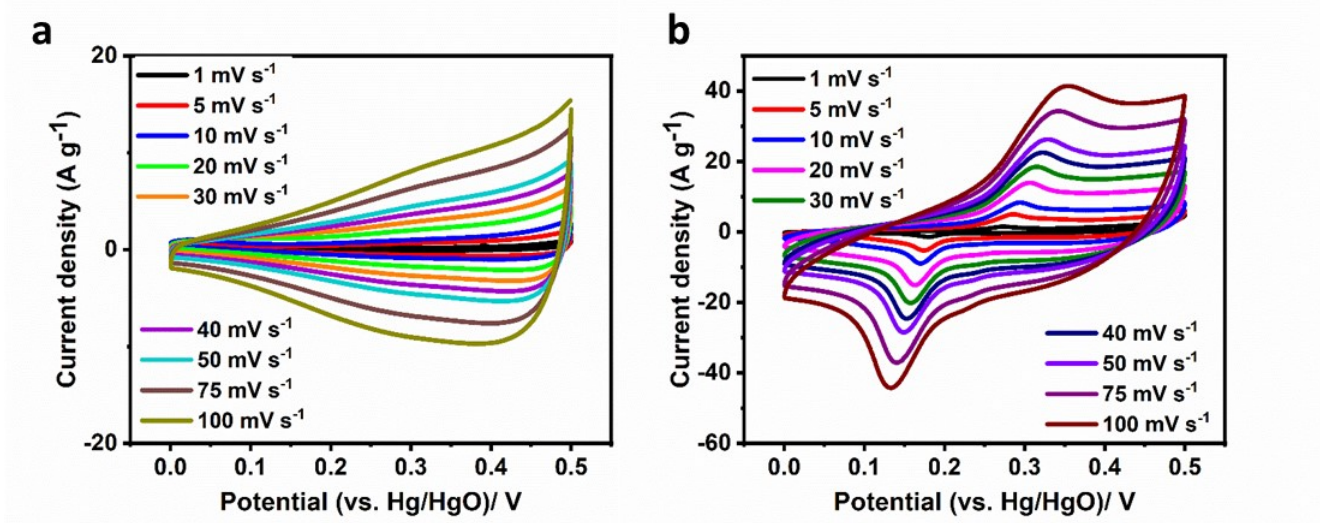
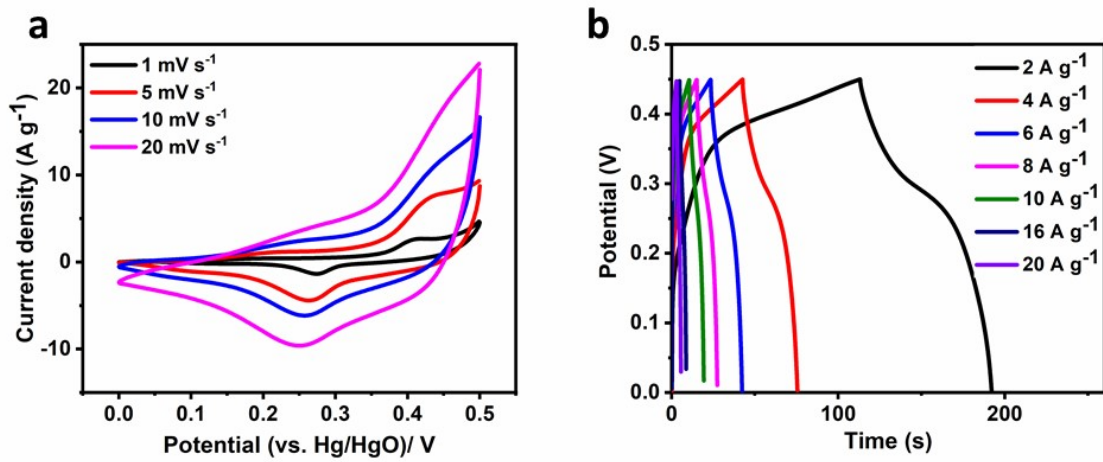
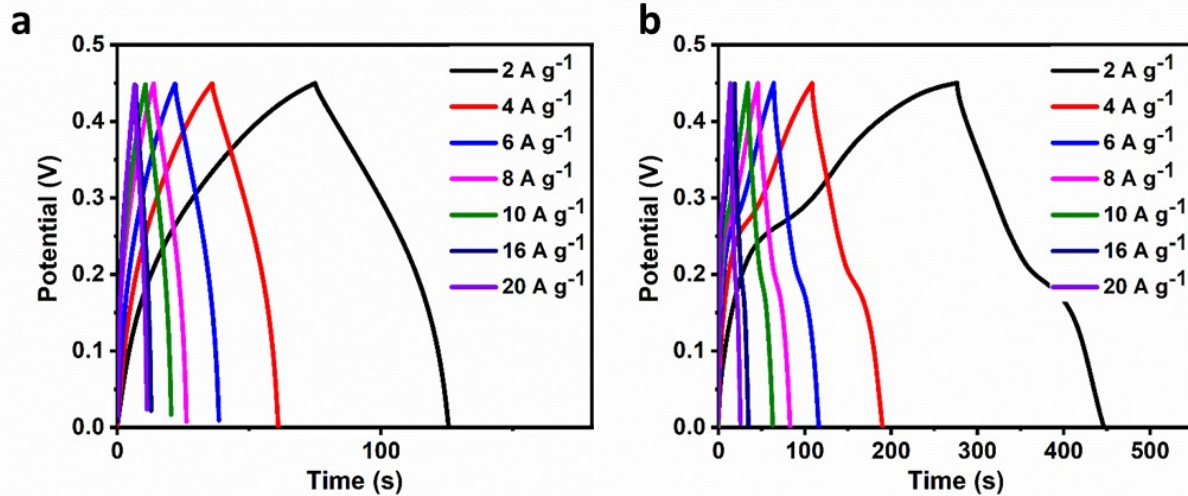


Figure S8 (a) CV curves at different scan rates (a) CuO NWAs and (b) Ni-Co-ZIF@CuO.



**Figure S9** (a) CV curves at different scan rates and (b) GCD curves at different current densities of powdery Ni-Co-ZIF.



**Figure S10** GCD curves at different current densities (a) CuO NWs and (b) Ni-Co-ZIF@CuO.

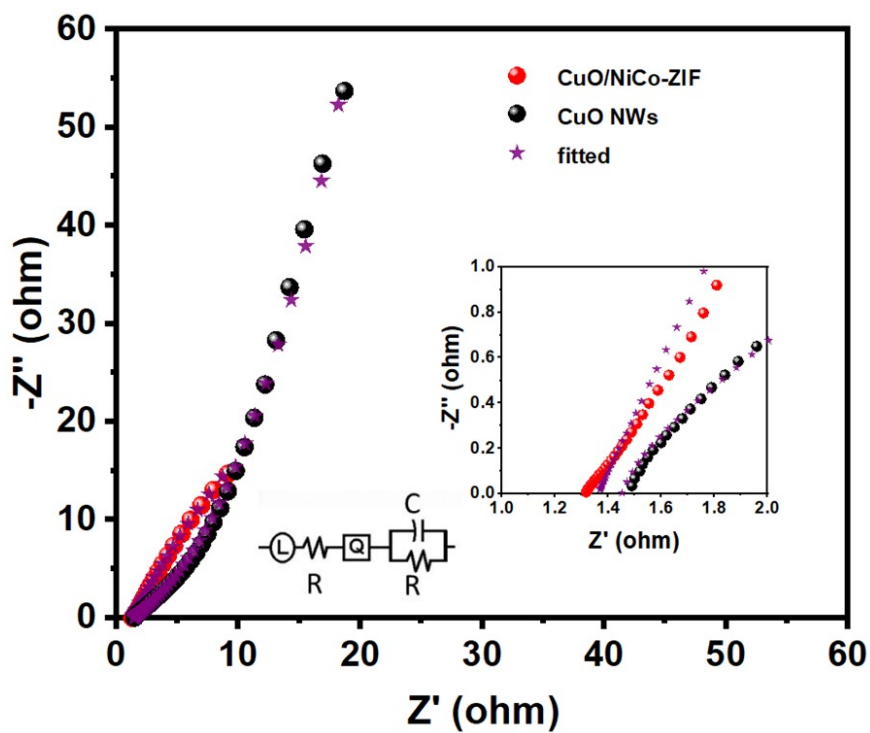


**Figure S11** Nyquist plot of the CuO NWs and Ni-Co-ZIF@CuO.

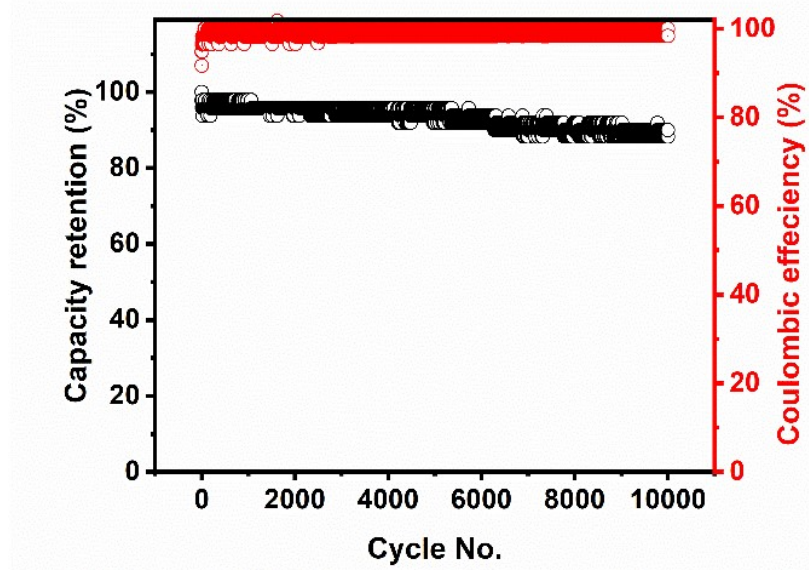


**Figure S12 (a)** Cycling stability of the CuO NWs at  $20 \text{ A g}^{-1}$ .

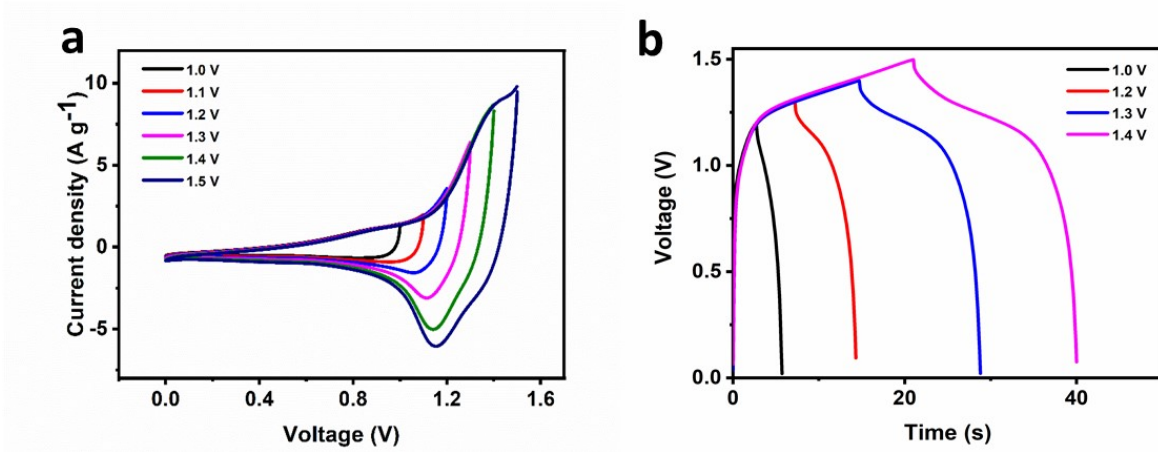


**Figure S13** (a) CV curves at same scan rate of  $50 \text{ mV s}^{-1}$  and (b) GCD curves at current density of  $6 \text{ A g}^{-1}$  of ASC device at different voltage window.

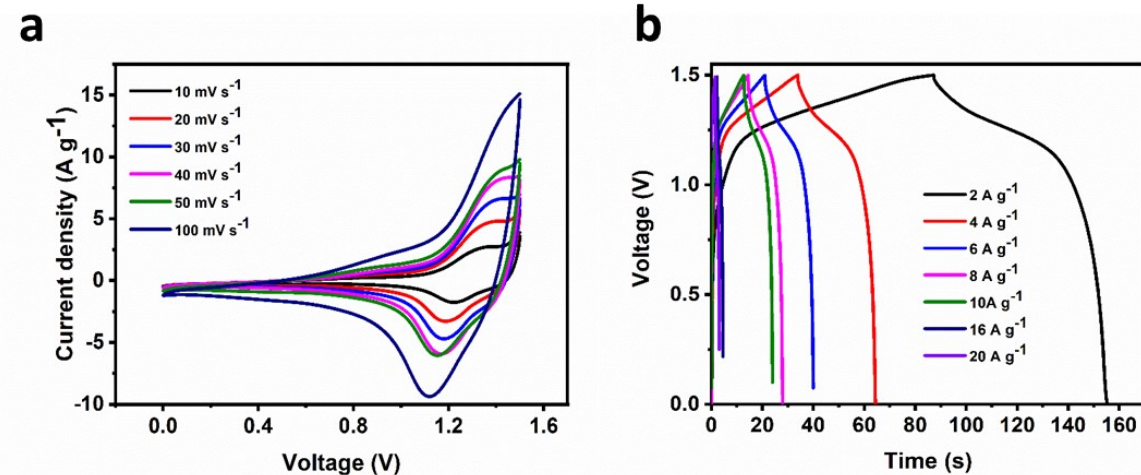


**Figure S14** (a) CV curves at different scan rates (b) GCD curves at different current densities of ASC device.

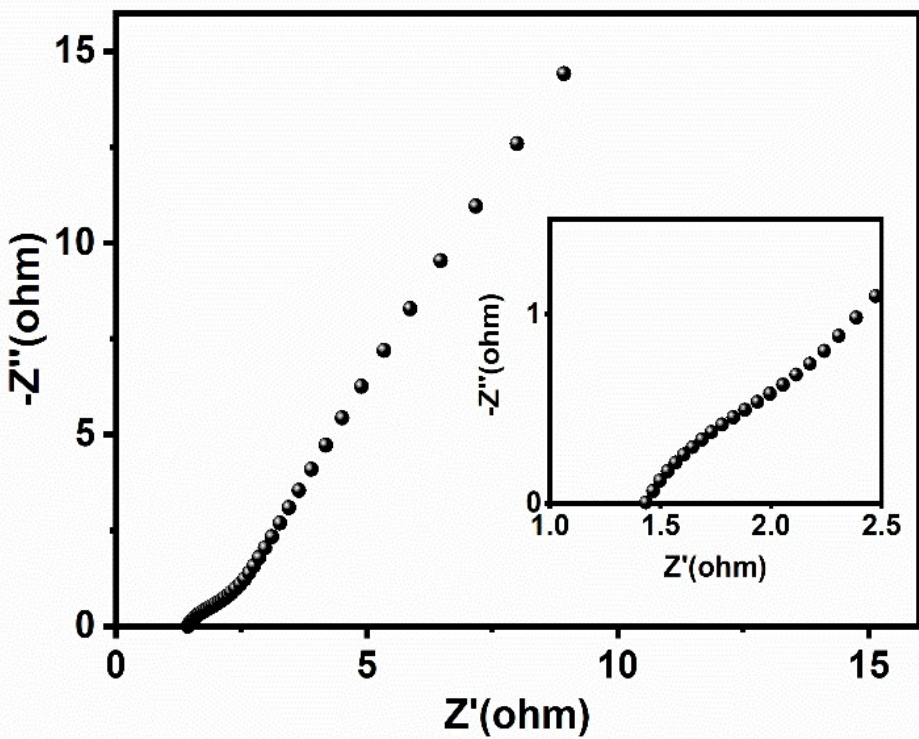


**Figure S15** (a) Nyquist plot of ASC device.

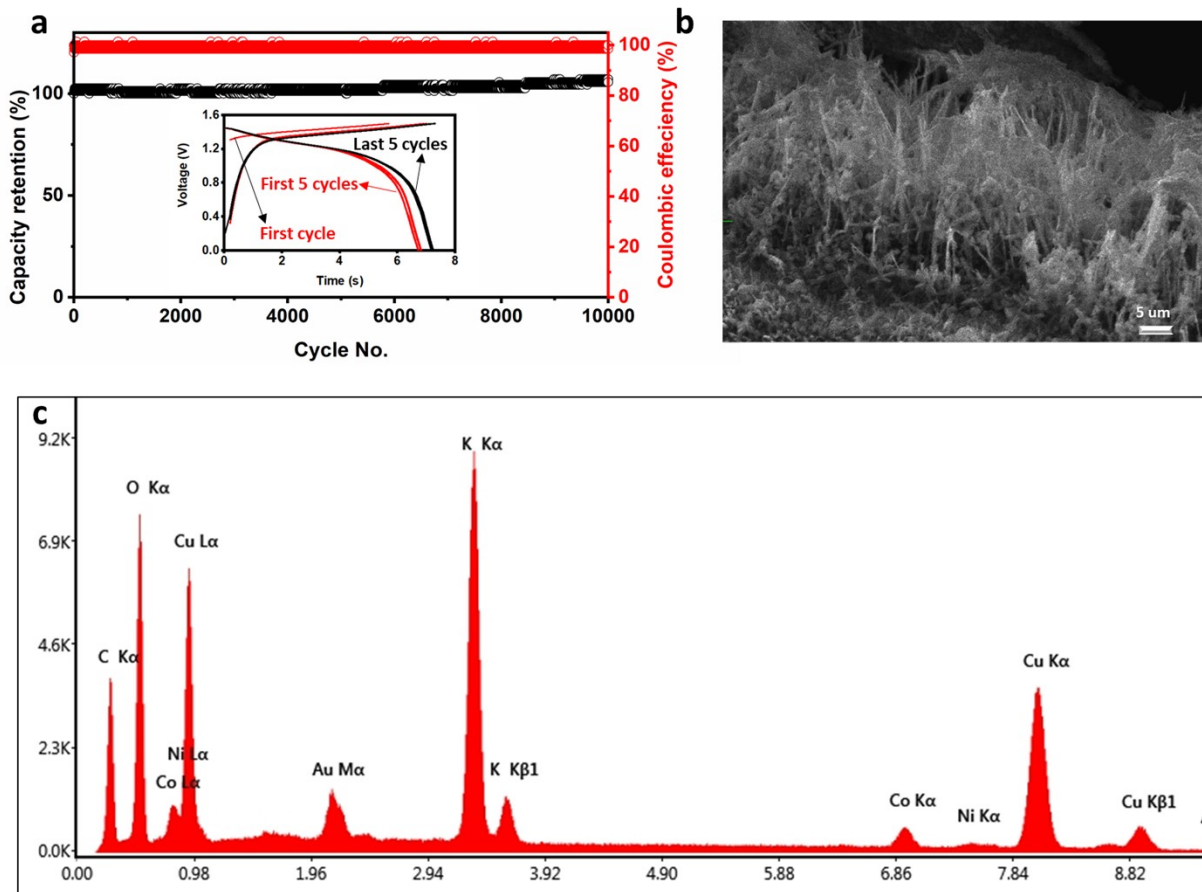


**Figure S16.** (a) Cycling stability of the ASC device during 10,000 cycle at current density of  $20 \text{ A g}^{-1}$ , (b) SEM image, and (c) EDX spectra of Ni-Co-ZIF@CuO after 10,000 cycles.

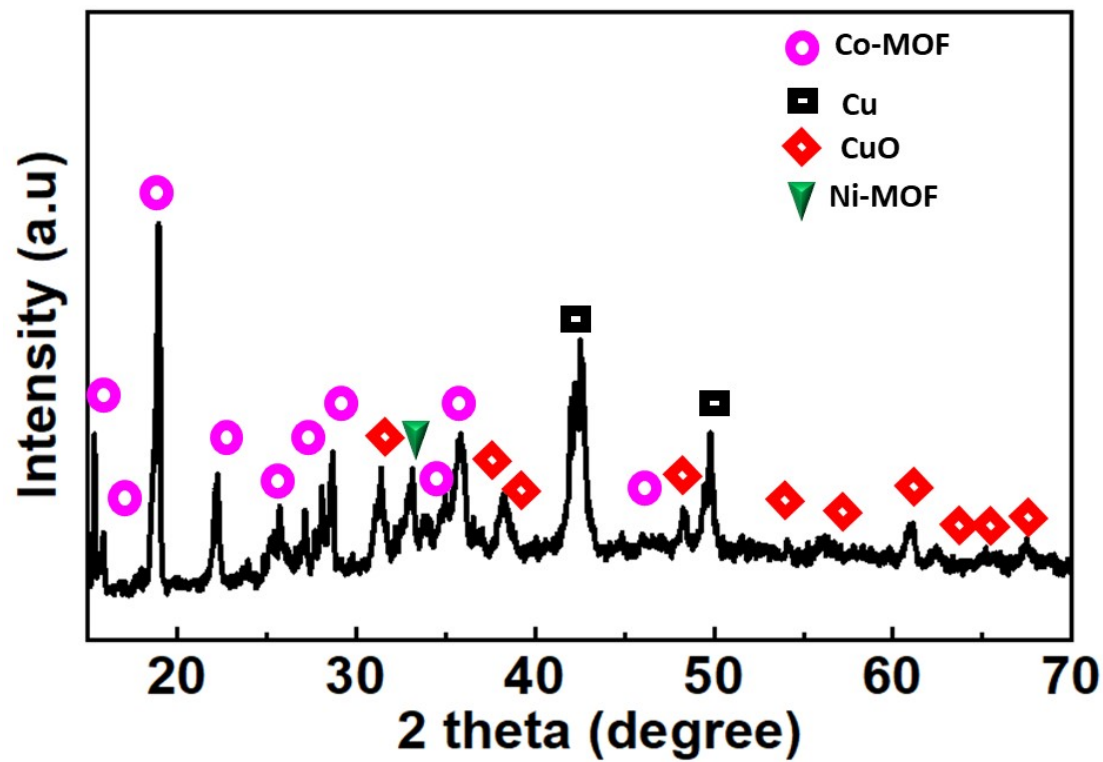


**Figure S17.** XRD spectra of Ni-Co-ZIF@CuO after 10,000 cycles.

## Part IV. Supplementary Tables

**Table S1.** Rate capability and detailed specific capacitances/capacities of Ni-Co-ZIF@CuO and CuO.

<b>Current density</b>	<b>Specific capacitance</b>		<b>Specific capacity</b>
	<b>A g<sup>-1</sup></b>	<b>F g<sup>-1</sup></b>	<b>C g<sup>-1</sup></b>
	<b>Ni-Co-ZIF@CuO</b>		<b>CuO</b>
<b>2</b>	756		340
<b>4</b>	729		328
<b>6</b>	693		312
<b>8</b>	658		296
<b>10</b>	645		290
<b>16</b>	569		256
<b>20</b>	516		232
<b>Rate capability</b>	68%		68%

**Table S2.** Detailed specific capacities of Ni-Co-ZIF@CuO with reported data.

<b>Electrode material</b>	<b>Specific capacitance</b>	<b>Current density</b>	<b>Electrolyte</b>	<b>Ref.</b>
	(F g <sup>-1</sup> )	(A g <sup>-1</sup> )		
Ni-MOF	306 F g <sup>-1</sup>	0.5 A g <sup>-1</sup>	1 M LiOH	15

Ni/Co-MOF	530 F g <sup>-1</sup>	0.5 A g <sup>-1</sup>	1 M LiOH	15
Co-MOF	220 F g <sup>-1</sup>	1 A g <sup>-1</sup>	6 M KOH	16
Co-MOF-RGO	430 F g <sup>-1</sup>	1 A g <sup>-1</sup>	6 M KOH	16
Ni-MOF	280 F g <sup>-1</sup>	1 A g <sup>-1</sup>	6 M KOH	16
Ni/Co-MOF	650 F g <sup>-1</sup>	1 A g <sup>-1</sup>	6 M KOH	16
Ni-doped MOF-5	380 F g <sup>-1</sup>	0.5 A g <sup>-1</sup>	1 M KOH	17
Co-MOF films	207 F g <sup>-1</sup>	0.6 A g <sup>-1</sup>	1 M LiOH	18
Co-BPDC	179 F g <sup>-1</sup>	NA	0.5 M LiOH	19
Co-MOF (SNNU-80)	106 F g <sup>-1</sup>	1 A g <sup>-1</sup>	1 M KOH	20
Ni/Co-MOF	530.4 F g <sup>-1</sup>	0.5 A g <sup>-1</sup>	1 M LiOH	21
Pillar Ni-MOF	552 F g <sup>-1</sup>	1 A g <sup>-1</sup>	2 M KOH	22
Ni-MOF	726 F g <sup>-1</sup>	1 A g <sup>-1</sup>	2 M KOH	23
Ni-Co-MOF/GO-2	447 F g <sup>-1</sup>	1 A g <sup>-1</sup>	6 M KOH	24
Ni-MOF	606 F g <sup>-1</sup>	1 A g <sup>-1</sup>	3 M KOH	25
MOF-derived NiO	473 F g <sup>-1</sup>	0.5 A g <sup>-1</sup>	3 M KOH	26
MOF-derived $\alpha$ -NiS	744 F g <sup>-1</sup>	1 A g <sup>-1</sup>	2 M KOH	27
NiO/C@CNF	742.2 F g <sup>-1</sup>	1 A g <sup>-1</sup>	3 M KOH	28
Ni-MOF	318 F g <sup>-1</sup>	1 A g <sup>-1</sup>	3 M KOH	29
<b>NiCo-ZIF@CuO</b>	<b>756 F g<sup>-1</sup> (340 C g<sup>-1</sup>)</b>	<b>2 A g<sup>-1</sup></b>	<b>3 M KOH</b>	<b>This work</b>

**Table S3.** Comparison of stability of Ni-Co-ZIF@CuO electrode material with reported data.

Electrode material	Capacity retention	Number of cycles	Ref.
	(%)		
Ni(OH) <sub>2</sub> /graphene	94	3,000	30
MnO <sub>2</sub> @NiCo-LDH	78	2,000	31
MnO <sub>2</sub> @NiCo-LDH/CoS <sub>2</sub>	58	2,000	31
NiOOH /GS hydrogels	85	8,000	32
Ni-MOF/CNT	95	5,000	33
Amorphous Ni(OH) <sub>2</sub> nanospheres	97	5,000	34
3D interconnected Ni(OH) <sub>2</sub> /UGF	63	10,000	35
Cu-MOF/rGO	92	1,000	36
NiCo <sub>2</sub> O <sub>4</sub> nanosheets	95	2,200	37
Porous NiCo <sub>2</sub> O <sub>4</sub> nanowires	93	3,000	38
Mesoporous Ni <sub>0.3</sub> Co <sub>2.7</sub> O <sub>4</sub>	98	3,000	39
NiCo <sub>2</sub> O <sub>4</sub> nanoplates	89	2,200	40
NiCo <sub>2</sub> O <sub>4</sub> nanowires	98	3,000	41
CuCo <sub>2</sub> O <sub>4</sub> mesoporous nanowires	79	5,000	42
CuCo <sub>2</sub> O <sub>4</sub> nanograss	94	5,000	43
CuCo <sub>2</sub> O <sub>4</sub> @MnO <sub>2</sub> on carbon fibers	90	5,000	44
CuCo <sub>2</sub> O <sub>4</sub> /CuO nanowire	95	5,000	45
<b>Ni-Co-ZIF@CuO</b>	<b>94</b>	<b>10,000</b>	<b>This work</b>

**Table S4.** Rate capability and detailed specific capacities of Ni-Co-ZIF@CuO//rGO ASC device.

Current density <b>A g<sup>-1</sup></b>	Specific capacity <b>C g<sup>-1</sup></b>	NiCo-ZIF@CuO//rGO
<b>2</b>	210	
<b>4</b>	186	
<b>6</b>	173	
<b>8</b>	162	
<b>10</b>	160	
<b>Rate capability</b>	76%	

**Table S5.** Comparison of specific capacitance/capacity of Ni-Co-ZIF@CuO//rGO ASC device with reported SC devices.

Device	Specific capacitance (F g <sup>-1</sup> )	Current density (A g <sup>-1</sup> )	Electrolyte	Ref.
NiO/C@CNF//AC	175 F g <sup>-1</sup>	1 A g <sup>-1</sup>	3 M KOH	28
Ni-MOF@NiS <sub>2</sub> // AC	84.84 F g <sup>-1</sup>	2 A g <sup>-1</sup>	KOH/PVA	46
Ni/Co-MOF-1//AC	157 F g <sup>-1</sup>	1 A g <sup>-1</sup>	6 M KOH	47
Ni-MOF 1–6//AC	87 F g <sup>-1</sup>	0.5 A g <sup>-1</sup>	3 M KOH	48

NixPoyOz(MOF derived)				
//NixPoyOz(MOF derived)	58 F g <sup>-1</sup>	1 A g <sup>-1</sup>	2M KOH	49
Co–Co LDH (MOF derived)/G//AC	116.6 F g <sup>-1</sup>	0.6 A g <sup>-1</sup>	1 M KOH	50
Ni–CoLDH/G (MOF derived) //AC	170.9 F g <sup>-1</sup>	0.7 A g <sup>-1</sup>	1 M KOH	51
NiCo <sub>2</sub> O <sub>4</sub> /β-NixCo1-x(OH) <sub>2</sub> / αNixCo1-x(OH) <sub>2</sub> (Co/Ni MOF derived)//AC	104 F g <sup>-1</sup>	1 A g <sup>-1</sup>	6 M KOH	52
Ni/Co-MOF//AC	58.8 F g <sup>-1</sup>	1 A g <sup>-1</sup>	2 M KOH	53
MnCo <sub>2</sub> S <sub>4</sub> /Co <sub>9</sub> S <sub>8</sub> //AC	128.8 F g <sup>-1</sup>	1 A g <sup>-1</sup>	6 M KOH	54
CoNi-DH-S@CC//ACF	136.5 F g <sup>-1</sup>	1 mA cm <sup>-2</sup>	PVA/KOH	55
Ni-Co-S-W)//AC	155 F g <sup>-1</sup>	1 A g <sup>-1</sup>	6 M KOH	56
Ni <sub>3</sub> S <sub>4</sub> //AC	110.5 F g <sup>-1</sup>	1 A g <sup>-1</sup>	2 M KOH	57
MOF derived CoP//FeP <sub>4</sub>	170.4 F g <sup>-1</sup>	1 A g <sup>-1</sup>	PVA/KOH	58
MNCFT//ONCFT	46 F g <sup>-1</sup>	1 mV s-1	PVA/H <sub>2</sub> SO <sub>4</sub>	59
HTNBs//AC	~ 100 F g <sup>-1</sup>	1 A g <sup>-1</sup>	6 M KOH	60
ZIF derived NiCoS@PPy//AC	97 F g <sup>-1</sup>	1 A g <sup>-1</sup>	2 M KOH	61
CP <sub>x</sub> /CO-40  NPC@rGO	~38 F g <sup>-1</sup>	1 A g <sup>-1</sup>	2 M KOH	62
Co <sub>3</sub> O <sub>4</sub> @C-500//rGO	127 F g <sup>-1</sup>	1 A g <sup>-1</sup>	1 M KOH	63
α-CoMn <sub>0.05</sub> (OH) <sub>x</sub> /ZIF-67//AC	70.3 F g <sup>-1</sup>	500 mA g <sup>-1</sup>	3 M KOH	64
Cu <sub>x</sub> O-C/PANI//ZIF-8NPC	131.34 F g <sup>-1</sup>	2 A g <sup>-1</sup>	3 M KOH	65
CC/NiCoP@NiCo-LDH//AC	125 F g <sup>-1</sup>	2 A g <sup>-1</sup>	PVA/KOH	66
P-(Ni,Co)Se <sub>2</sub> //ZC	100 F g <sup>-1</sup>	0.5 A g <sup>-1</sup>	PVA/KOH	67
NiCoMn-OH//AC	121.5 F g <sup>-1</sup>	1 A g <sup>-1</sup>	PVA/KOH	68
ZZN-2//AC	129.5 F g <sup>-1</sup>	1 A g <sup>-1</sup>	PVA/KOH	69

<b>Ni-Co-ZIF@CuO//rGO</b>	<b>140 F g<sup>-1</sup></b> <b>210 C g<sup>-1</sup></b>	<b>2 A g<sup>-1</sup></b>	<b>3M KOH</b>	<b>This work</b>
---------------------------	--	---------------------------	---------------	------------------

**Table S6.** Comparison of energy and power densities of Ni-Co-ZIF@CuO//rGO ASC device with reported SC devices.

<b>Device</b>	<b>Energy density (Wh kg<sup>-1</sup>)</b>	<b>Power density (kW kg<sup>-1</sup>)</b>	<b>Ref.</b>
NixPoyOz(Ni-MOF derived) //	7.95	0.5	49
NixPoyOz(Ni-MOF derived)			
MnCo2S4/Co9S8//AC	45.8	0.8	54
Ni <sub>3</sub> S <sub>4</sub> //AC	18.625	1.5	57
Co <sub>3</sub> O <sub>4</sub> @C-500//rGO	43.99	0.824	63
NP-150//AC	32.02	0.7	70
CoS-NP/CoS-NS DSNB//AC	39.9	0.756	71
Co <sub>9</sub> S <sub>8</sub> /AC	31.4	0.2	72
NiO@CNT//PCPs	25.4	400	73
NSCGH//AC	21.1	0.3	74
m-Nb <sub>2</sub> O <sub>5</sub> -C//MSP-20	20	12.137	75
C/T-Nb <sub>2</sub> O <sub>5</sub> nanowires//AC	43.4	0.374	76
Nb <sub>2</sub> O <sub>5</sub> @MC/MCHS	38	0.32	77
CNT/Nb <sub>2</sub> O <sub>5</sub> //AC	33.5	0.082	78
MOF derived Ni-Co-S/?ACC	30.1	0.8	79

(Ni <sub>0.1</sub> Co <sub>0.9</sub> ) <sub>9</sub> Se <sub>8</sub> //rGO	17	3.1	80
NiCo <sub>2</sub> S <sub>4</sub> /MWCNTs//rGO	13.4	0.75	81
C-NiCo <sub>2</sub> S <sub>4</sub> //AC	38.3	0.8	12
MOF derived C/NG-A//C/NG-A	33.89	500	82
ZIF-8/CNTs//N-C/CNTs	23	0.847	83
Ni <sub>3</sub> S <sub>2</sub> MWCNTs//AC	19.8	0.798	84
NiCoP/NiCo-OH30//PC	34	0.775	85
NiCoP//AC	32	1.301	86
NiCoP-CoP//PNGF	39	1.784	87
NiCoP/NiCo-OH//PC	34	0.775	88
NCLP@NiMn-LDH//AC	42	0.750	89
NiSe <sub>2</sub> @CNT//AC	25.61	0.810	90
<b>Ni-Co-ZIF@CuO//rGO</b>	<b>43</b>	<b>2.242</b>	<b>This work</b>

**Table S7.** Comparison of capacity retention of ASC (Ni-Co-ZIF@CuO//rGO) device with reported devices.

Device	Capacity Retention (%)	No. of Cycles	Ref.
MoS <sub>2</sub> -ZIF//ZDPC	81	10,000	91
Co-MOF//AC	69.7	2,000	92
MOF-derived CoNi <sub>2</sub> S <sub>4</sub> //YS-C	63.18	5,000	93
MOXC-700//NPC	80	10,000	94
MOF-NPC/MnO <sub>2</sub> //MOF-NPC	87.3	9,000	95

MSCs//MSCs	96.0	10,000	96
Co <sub>3</sub> O <sub>4</sub> //carbon	89	2,000	97
rGO/MoO <sub>3</sub> //rGO/MoO <sub>3</sub>	80	5,000	98
MOF-derived P-Co <sub>3</sub> O <sub>4</sub> @PNC// PNC	96.8	10,000	99
MOF-derived MnCo <sub>2</sub> S <sub>4</sub> /Co <sub>9</sub> S <sub>8</sub> // AC	94.8	5,000	54
Ni/Co-MOF-1//AC	61	4,000	47
GA@UiO-66-NH <sub>2</sub> //Ti <sub>3</sub> C <sub>2</sub> T <sub>X</sub> MXene	88	10,000	100
MOF derived Cu(Co-Ni) <sub>2</sub> S <sub>4</sub> NTs//PC	95.8	5,000	101
Li <sub>4</sub> Ti <sub>5</sub> O <sub>12</sub> //MOFDC	82	10,000	102
NiO@Co <sub>3</sub> O <sub>4</sub> @GQDs//AC	97.5	2,000	103
NC12//NBO	95.6	5,000	104
CoO@NiO/ACT//Graphene/ACT	84	10,000	105
<b>CuO/Zn-Co-ZIF//rGO</b>	<b>105 %</b>	<b>10,000</b>	<b>This work</b>

## References

1. X. Jiang, T. Herricks and Y. Xia, *Nano letters*, 2002, **2**, 1333-1338.
2. Y. Zhu, W. Du, Q. Zhang, H. Yang, Q. Zong, Q. Wang, Z. Zhou and J. Zhan, *Chemical Communications*, 2020, **56**, 13848-13851.
3. G. Kresse and J. Furthmüller, *Physical review B*, 1996, **54**, 11169.
4. G. Kresse and J. Furthmüller, *Computational materials science*, 1996, **6**, 15-50.
5. P. E. Blöchl, *Physical review B*, 1994, **50**, 17953.
6. G. Kresse and D. Joubert, *Physical review b*, 1999, **59**, 1758.
7. J. P. Perdew, K. Burke and M. Ernzerhof, *Physical review letters*, 1996, **77**, 3865.
8. H. J. Monkhorst and J. D. Pack, *Physical review B*, 1976, **13**, 5188.
9. S. Grimme, *Journal of computational chemistry*, 2006, **27**, 1787-1799.
10. I. Hussain, A. Ali, C. Lamiel, S. G. Mohamed, S. Sahoo and J.-J. Shim, *Dalton Transactions*, 2019, **48**, 3853-3861.
11. I. Hussain, S. G. Mohamed, A. Ali, N. Abbas, S. M. Ammar and W. Al Zoubi, *Journal of Electroanalytical Chemistry*, 2019, **837**, 39-47.
12. S. G. Mohamed, I. Hussain and J.-J. Shim, *Nanoscale*, 2018, **10**, 6620-6628.
13. I. Hussain, C. Lamiel, S. G. Mohamed, S. Vijayakumar, A. Ali and J.-J. Shim, *Journal of industrial and*

- engineering chemistry*, 2019, **71**, 250-259.
14. I. Hussain, J. M. Lee, S. Iqbal, H. S. Kim, S. W. Jang, J. Y. Jung, H. J. An, C. Lamiel, S. G. Mohamed and Y. R. Lee, *Electrochimica Acta*, 2020, 135953.
15. H. Xia, J. Zhang, Z. Yang, S. Guo, S. Guo and Q. Xu, *Nano-micro letters*, 2017, **9**, 1-11.
16. M. S. Rahmanifar, H. Hesari, A. Noori, M. Y. Masoomi, A. Morsali and M. F. Mousavi, *Electrochimica Acta*, 2018, **275**, 76-86.
17. P. C. Banerjee, D. E. Lobo, R. Middag, W. K. Ng, M. E. Shaibani and M. Majumder, *ACS Applied Materials & Interfaces*, 2015, **7**, 3655-3664.
18. D. Y. Lee, S. J. Yoon, N. K. Shrestha, S.-H. Lee, H. Ahn and S.-H. Han, *Microporous and Mesoporous Materials*, 2012, **153**, 163-165.
19. D. Y. Lee, D. V. Shinde, E.-K. Kim, W. Lee, I.-W. Oh, N. K. Shrestha, J. K. Lee and S.-H. Han, *Microporous and mesoporous materials*, 2013, **171**, 53-57.
20. X.-Y. Hou, X. Wang, S.-N. Li, Y.-C. Jiang, M.-C. Hu and Q.-G. Zhai, *Crystal Growth & Design*, 2017, **17**, 3229-3235.
21. H. Xia, J. Zhang, Z. Yang, S. Guo, S. Guo and Q. Xu, *Nano-Micro Letters*, 2017, **9**.
22. C. Qu, Y. Jiao, B. Zhao, D. Chen, R. Zou, K. S. Walton and M. Liu, *Nano Energy*, 2016, **26**, 66-73.
23. L. Kang, S.-X. Sun, L.-B. Kong, J.-W. Lang and Y.-C. Luo, *Chinese Chemical Letters*, 2014, **25**, 957-961.
24. J. Hong, S.-J. Park and S. Kim, *Electrochimica Acta*, 2019, **311**, 62-71.
25. Y. Xiao, W. Wei, M. Zhang, S. Jiao, Y. Shi and S. Ding, *ACS Applied Energy Materials*, 2019, **2**, 2169-2177.
26. M. K. Wu, C. Chen, J. J. Zhou, F. Y. Yi, K. Tao and L. Han, *Journal of Alloys and Compounds*, 2018, **734**, 1-8.
27. C. Qu, L. Zhang, W. Meng, Z. Liang, B. Zhu, D. Dang, S. Dai, B. Zhao, H. Tabassum and S. Gao, *Journal of Materials Chemistry A*, 2018, **6**, 4003-4012.
28. S. Shin and M. W. Shin, *Applied Surface Science*, 2021, **540**, 148295.
29. H. Wang, C. Zhu, M. Wu, F. Zheng, Y. Gao and H. Niu, *Journal of Materials Science*, 2021, **56**, 2517-2527.
30. J. Yan, Z. Fan, W. Sun, G. Ning, T. Wei, Q. Zhang, R. Zhang, L. Zhi and F. Wei, *Advanced Functional Materials*, 2012, **22**, 2632-2641.
31. X. Wang, F. Huang, F. Rong, P. He and R. Que, *Journal of Materials Chemistry A*, 2019, **7**, 12018-12028.
32. R. Wang, C. Xu and J.-M. Lee, *Nano Energy*, 2016, **19**, 210-221.
33. P. Wen, P. Gong, J. Sun, J. Wang and S. Yang, *J. Mater. Chem. A*, 2015, **3**, 13874-13883.
34. H. Li, M. Yu, F. Wang, P. Liu, Y. Liang, J. Xiao, C. Wang, Y. Tong and G. Yang, *Nature communications*, 2013, **4**, 1894.
35. J. Ji, L. L. Zhang, H. Ji, Y. Li, X. Zhao, X. Bai, X. Fan, F. Zhang and R. S. Ruoff, *ACS nano*, 2013, **7**, 6237-6243.
36. M. Saraf, R. Rajak and S. M. Mobin, *Journal of Materials Chemistry A*, 2016, **4**, 16432-16445.
37. H. Wang and X. Wang, *ACS applied materials & interfaces*, 2013, **5**, 6255-6260.
38. H. Jiang, J. Ma and C. Li, *Chemical communications*, 2012, **48**, 4465-4467.
39. H. B. Wu, H. Pang and X. W. D. Lou, *Energy & Environmental Science*, 2013, **6**, 3619-3626.
40. J. Pu, J. Wang, X. Jin, F. Cui, E. Sheng and Z. Wang, *Electrochimica Acta*, 2013, **106**, 226-234.
41. H. Wang, Q. Gao and L. Jiang, *small*, 2011, **7**, 2454-2459.
42. S. Liu, D. Ni, H.-F. Li, K. N. Hui, C.-Y. Ouyang and S. C. Jun, *Journal of Materials Chemistry A*, 2018, **6**, 10674-10685.
43. J. Cheng, H. Yan, Y. Lu, K. Qiu, X. Hou, J. Xu, L. Han, X. Liu, J.-K. Kim and Y. Luo, *Journal of Materials Chemistry A*, 2015, **3**, 9769-9776.
44. Q. Wang, J. Xu, X. Wang, B. Liu, X. Hou, G. Yu, P. Wang, D. Chen and G. Shen, *ChemElectroChem*, 2014, **1**, 559-564.
45. Y. Wang, C. Shen, L. Niu, R. Li, H. Guo, Y. Shi, C. Li, X. Liu and Y. Gong, *Journal of Materials Chemistry A*, 2016, **4**, 9977-9985.
46. J. Zhang, Y. Li, M. Han, Q. Xia, Q. Chen and M. Chen, *Materials Research Bulletin*, 2021, **137**, 111186.
47. X. Zhang, N. Qu, S. Yang, D. Lei, A. Liu and Q. Zhou, *Materials Chemistry Frontiers*, 2021, **5**, 482-491.
48. P. Du, Y. Dong, C. Liu, W. Wei, D. Liu and P. Liu, *Journal of Colloid and Interface Science*, 2018, **518**, 57-68.
49. R. Bendi, V. Kumar, V. Bhavanasi, K. Parida and P. S. Lee, *Advanced Energy Materials*, 2016, **6**, 1501833.
50. X. Bai, J. Liu, Q. Liu, R. Chen, X. Jing, B. Li and J. Wang, *Chemistry—A European Journal*, 2017, **23**, 14839-14847.
51. X. Bai, Q. Liu, Z. Lu, J. Liu, R. Chen, R. Li, D. Song, X. Jing, P. Liu and J. Wang, *ACS Sustainable Chemistry & Engineering*, 2017, **5**, 9923-9934.

52. H. Mei, Y. Mei, S. Zhang, Z. Xiao, B. Xu, H. Zhang, L. Fan, Z. Huang, W. Kang and D. Sun, *Inorganic chemistry*, 2018, **57**, 10953-10960.
53. S. Gao, Y. Sui, F. Wei, J. Qi, Q. Meng, Y. Ren and Y. He, *Journal of colloid and interface science*, 2018, **531**, 83-90.
54. H. Jia, J. Wang, W. Fu, J. Hu and Y. Liu, *Chemical Engineering Journal*, 2020, **391**, 123541.
55. Y. Wu, H. Chen, Y. Lu, J. Yang, X. Zhu, Y. Zheng, G. Lou, Y. Wu, Q. Wu and Z. Shen, *Journal of Colloid and Interface Science*, 2021, **581**, 455-464.
56. W. He, Z. Liang, K. Ji, Q. Sun, T. Zhai and X. Xu, *Nano Research*, 2018, **11**, 1415-1425.
57. H. Wang, M. Liang, D. Duan, W. Shi, Y. Song and Z. Sun, *Chemical Engineering Journal*, 2018, **350**, 523-533.
58. X. Wei, Y. Song, L. Song, X. D. Liu, Y. Li, S. Yao, P. Xiao and Y. Zhang, *Small*, 2021, **17**, 2007062.
59. Y. Wang, X. Wang, X. Li, X. Li, Y. Liu, Y. Bai, H. Xiao and G. Yuan, *Advanced Functional Materials*, 2021, **31**, 2008185.
60. M. Feng, J. Gu, G. C. Zhang, M. Xu, Y. Yu, X. Liu, Z. Wang, B. Yin, Y. Liu and S. Liu, *Journal of Solid State Chemistry*, 2020, **282**, 121084.
61. X. Zhao, Q. Ma, K. Tao and L. Han, *ACS Applied Energy Materials*, 2021, **4**, 4199-4207.
62. S. Gayathri, P. Arunkumar, D. Saha and J. H. Han, *Journal of Colloid and Interface Science*, 2021, **588**, 557-570.
63. T. Shu, H. Wang, Q. Li, Z. Feng, F. Wei, K. X. Yao, Z. Sun, J. Qi and Y. Sui, *Chemical Engineering Journal*, 2021, **419**, 129631.
64. C. Liu, Y. Bai, J. Wang, Z. Qiu and H. Pang, *Journal of Materials Chemistry A*, 2021.
65. K. Chhetri, B. Dahal, T. Mukhiya, A. P. Tiwari, A. Muthurasu, T. Kim, H. Kim and H. Y. Kim, *Carbon*, 2021, **179**, 89-99.
66. X. Gao, Y. Zhao, K. Dai, J. Wang, B. Zhang and X. Shen, *Chemical Engineering Journal*, 2020, **384**, 123373.
67. Q. Zong, Y. Zhu, Q. Wang, H. Yang, Q. Zhang, J. Zhan and W. Du, *Chemical Engineering Journal*, 2020, **392**, 123664.
68. Y. Du, G. Li, M. Chen, X. Yang, L. Ye, X. Liu and L. Zhao, *Chemical Engineering Journal*, 2019, **378**.
69. C. Huang, C. Hao, Z. Ye, S. Zhou, X. Wang, L. Zhu and J. Wu, *Nanoscale*, 2019, **11**, 10114-10128.
70. S. Hou, X. Xu, M. Wang, Y. Xu, T. Lu, Y. Yao and L. Pan, *Journal of Materials Chemistry A*, 2017, **5**, 19054-19061.
71. H. Hu, B. Y. Guan and X. W. D. Lou, *Chem*, 2016, **1**, 102-113.
72. R. Rakhi, N. A. Alhebshi, D. H. Anjum and H. N. Alshareef, *Journal of Materials Chemistry A*, 2014, **2**, 16190-16198.
73. H. Yi, H. Wang, Y. Jing, T. Peng and X. Wang, *Journal of Power Sources*, 2015, **285**, 281-290.
74. X. Yu, B. Lu and Z. Xu, *Advanced materials*, 2014, **26**, 1044-1051.
75. E. Lim, H. Kim, C. Jo, J. Chun, K. Ku, S. Kim, H. I. Lee, I.-S. Nam, S. Yoon and K. Kang, *ACS nano*, 2014, **8**, 8968-8978.
76. X. Wang, C. Yan, J. Yan, A. Sumboja and P. S. Lee, *Nano Energy*, 2015, **11**, 765-772.
77. S. Zhang, J. Wu, J. Wang, W. Qiao, D. Long and L. Ling, *Journal of Power Sources*, 2018, **396**, 88-94.
78. X. Wang, G. Li, Z. Chen, V. Augustyn, X. Ma, G. Wang, B. Dunn and Y. Lu, *Advanced Energy Materials*, 2011, **1**, 1089-1093.
79. W. Zhao, Y. Zheng, L. Cui, D. Jia, D. Wei, R. Zheng, C. Barrow, W. Yang and J. Liu, *Chemical Engineering Journal*, 2019, **371**, 461-469.
80. P. Yang, Z. Wu, Y. Jiang, Z. Pan, W. Tian, L. Jiang and L. Hu, *Advanced Energy Materials*, 2018, **8**, 1801392.
81. Q. Gao, X. Wang, Z. Shi, Z. Ye, W. Wang, N. Zhang, Z. Hong and M. Zhi, *Chemical Engineering Journal*, 2018, **331**, 185-193.
82. W. Xia, C. Qu, Z. Liang, B. Zhao, S. Dai, B. Qiu, Y. Jiao, Q. Zhang, X. Huang, W. Guo, D. Dang, R. Zou, D. Xia, Q. Xu and M. Liu, *Nano Letters*, 2017, **17**, 2788-2795.
83. Y. Zhang, B. Lin, J. Wang, J. Tian, Y. Sun, X. Zhang and H. Yang, *Journal of Materials Chemistry A*, 2016, **4**, 10282-10293.
84. C.-S. Dai, P.-Y. Chien, J.-Y. Lin, S.-W. Chou, W.-K. Wu, P.-H. Li, K.-Y. Wu and T.-W. Lin, *ACS Applied Materials & Interfaces*, 2013, **5**, 12168-12174.
85. X. Li, H. Wu, A. M. Elshahawy, L. Wang, S. J. Pennycook, C. Guan and J. Wang, *Advanced Functional Materials*, 2018, **28**, 1800036.
86. H. Liang, C. Xia, Q. Jiang, A. N. Gandi, U. Schwingenschlögl and H. N. Alshareef, *Nano Energy*, 2017, **35**, 331-

- 340.
87. W. Song, J. Wu, G. Wang, S. Tang, G. Chen, M. Cui and X. Meng, *Advanced Functional Materials*, 2018, **28**, 1804620.
88. X. Li, H. Wu, A. M. Elshahawy, L. Wang, S. J. Pennycook, C. Guan and J. Wang, *Advanced Functional Materials*, 2018, **28**, 1800036.
89. H. Liang, J. Lin, H. Jia, S. Chen, J. Qi, J. Cao, T. Lin, W. Fei and J. Feng, *Journal of Materials Chemistry A*, 2018, **6**, 15040-15046.
90. Y. Zheng, Y. Tian, S. Sarwar, J. Luo and X. Zhang, *Journal of Power Sources*, 2020, **452**, 227793.
91. R. Wang, D. Jin, Y. Zhang, S. Wang, J. Lang, X. Yan and L. Zhang, *Journal of Materials Chemistry A*, 2017, **5**, 292-302.
92. G. Zhu, H. Wen, M. Ma, W. Wang, L. Yang, L. Wang, X. Shi, X. Cheng, X. Sun and Y. Yao, *Chemical Communications*, 2018, **54**, 10499-10502.
93. Q. Wang, F. Gao, B. Xu, F. Cai, F. Zhan, F. Gao and Q. Wang, *Chemical Engineering Journal*, 2017, **327**, 387-396.
94. A. Mahmood, R. Zou, Q. Wang, W. Xia, H. Tabassum, B. Qiu and R. Zhao, *ACS applied materials & interfaces*, 2016, **8**, 2148-2157.
95. M. Yao, X. Zhao, L. Jin, F. Zhao, J. Zhang, J. Dong and Q. Zhang, *Chemical Engineering Journal*, 2017, **322**, 582-589.
96. F. Dai, X. Wang, S. Zheng, J. Sun, Z. Huang, B. Xu, L. Fan, R. Wang, D. Sun and Z.-S. Wu, *Chemical Engineering Journal*, 2021, **413**, 127520.
97. R. R. Salunkhe, J. Tang, Y. Kamachi, T. Nakato, J. H. Kim and Y. Yamauchi, *ACS nano*, 2015, **9**, 6288-6296.
98. X. Cao, B. Zheng, W. Shi, J. Yang, Z. Fan, Z. Luo, X. Rui, B. Chen, Q. Yan and H. Zhang, *Advanced materials*, 2015, **27**, 4695-4701.
99. S. Liu, L. Kang, J. Zhang, E. Jung, S. Lee and S. C. Jun, *Energy Storage Materials*, 2020, **32**, 167-177.
100. K. Jayaramulu, M. Horn, A. Schneemann, H. Saini, A. Bakandritsos, V. Ranc, M. Petr, V. Stavila, C. Narayana, B. Scheibe, Š. Kment, M. Otyepka, N. Motta, D. Dubal, R. Zbořil and R. A. Fischer, *Advanced Materials*, 2021, **33**, 2004560.
101. G. Nagaraju, S. C. Sekhar, B. Ramulu and J. S. Yu, *Energy Storage Materials*, 2021, **35**, 750-760.
102. A. Banerjee, K. K. Upadhyay, D. Puthusseri, V. Aravindan, S. Madhavi and S. Ogale, *Nanoscale*, 2014, **6**, 4387-4394.
103. Z. Gao, N. Song and X. Li, *Journal of Materials Chemistry A*, 2015, **3**, 14833-14844.
104. J. Johnson William, I. Manohara Babu and G. Muralidharan, *Chemical Engineering Journal*, 2021, **422**, 130058.
105. X. Yin, C. Zhi, W. Sun, L.-P. Lv and Y. Wang, *Journal of Materials Chemistry A*, 2019, **7**, 7800-7814.